

Generation and Reaction of Vinyl Groups on a Cu(100) Surface

Michael X. Yang, Joseph Eng, Jr., Phillip W. Kash, George W. Flynn, and Brian E. Bent*

Department of Chemistry and Columbia Radiation Laboratory, Columbia University,
New York, New York 10027

Michael T. Holbrook and Simon R. Bare

The Dow Chemical Company, Midland, Michigan 48674

John L. Gland

Department of Chemistry, University of Michigan, Ann Arbor, Michigan 48109

Daniel A. Fischer

National Synchrotron Light Source, Brookhaven National Laboratory, Upton, New York 11973

Received: August 16, 1995; In Final Form: April 23, 1996[⊗]

The adsorption and reactions of vinyl bromide and vinyl iodide on a Cu(100) surface have been studied by temperature-programmed desorption in conjunction with near-edge X-ray absorption fine structure (NEXAFS) and work function change measurements. Vinyl bromide adsorbs molecularly on the surface at 100 K. The polarization dependence of the $\pi^*_{\text{C}=\text{C}}$ resonance indicates that the molecules lie with their π bond within $28 \pm 5^\circ$ of parallel to the surface. Upon heating, both vinyl bromide and vinyl iodide decompose to generate surface vinyl groups, which adopt a tilted orientation on the surface. Both the molecular halides and the surface vinyl groups show a splitting of the $\pi^*_{\text{C}=\text{C}}$ NEXAFS resonance due to the inequivalence of the carbon atoms in these species. The position of the $\sigma^*_{\text{C}-\text{C}}$ shape resonances for these species indicates little change ($<0.05 \text{ \AA}$) in C=C bond length due to adsorption and dissociation to form vinyl groups. Chemical displacement studies show that the C-Br bond cleavage in vinyl bromide occurs at 160 K. This dissociation temperature is confirmed by complementary NEXAFS and work function change measurement results. At 250 K, vinyl groups couple to yield 1,3-butadiene with 100% selectivity.

1. Introduction

While vinyl groups ($\text{CH}=\text{CH}_2$) have frequently been postulated as intermediates in surface processes, there have been surprisingly few studies in which these species have been isolated and characterized. From a mechanistic standpoint, the interest in vinyl ($\text{CH}=\text{CH}_2$) groups arises from their role as likely intermediates in the catalytic hydrogenation of acetylene and catalytic dehydrogenation of ethylene and vinyl halides. Vinyl groups have also attracted attention as possible intermediates in the conversion of ethylene to ethylidyne on Pt(111).¹ From a structural standpoint, vinyl groups are of interest as adsorbates with competing binding geometries. Specifically, competition is to be expected between end-on (η^1) coordination of vinyl to the metal surface through bonding with the hydrogen-deficient carbon atom and side-on (η^2) coordination of vinyl to the metal through the π bond. This competition between σ and π coordination is analogous to that found for phenyl (C_6H_5) groups, where a tilted orientation on Cu(111) surfaces was recently documented by NEXAFS.² Finally, from a reactivity standpoint, the chemistry of vinyl groups is of interest in comparison with that of phenyl, where unusual low-temperature coupling pathways (which appear to involve free radical mechanisms), in addition to much higher temperature metal-mediated coupling reactions, have been observed on copper surfaces.^{3,4}

To date, CHCH_2 groups have been proposed as stable surface fragments in ethylene decomposition on Ni(100),^{5–9} Pt(100),^{10,11} and Pd(100),¹² acetylene hydrogenation on Ni[5(111) \times (110)]¹³ and Ru(001),¹⁴ vinyl halide decomposition on Ag(111)¹⁵ and Pt(111),^{16–18} and electron-induced decomposition of ethylene on Ag(111).^{19,20} On Ni(100)^{5–9} and Pt(111),^{16–18} the surface CHCH_2 species have been classified as η^1 -vinyls on the basis of spectroscopic evidence [high-resolution electron energy loss spectroscopy (HREELS) and near-edge X-ray absorption fine structure (NEXAFS) measurements] for weak π interactions with the surface. In addition, these studies indicate that the η^1 -vinyl groups adopt a tilted orientation on the surface. It is likely that the CHCH_2 species on Ag(111) are also η^1 -coordinated on the basis of the weak π coordination found for olefins on this metal. On Pd(100)¹² and Ru(001),¹⁴ however, η^2 -vinylidene coordination has been proposed on the basis of HREELS results, which show an absence of C=C stretching modes above 1500 cm^{-1} .

In the context of the current studies on Cu(100), the results for the η^1 -vinyl systems are the most relevant. In these systems, the reactivity of surface vinyls is as follows: on Ag(111), vinyls couple to produce butadiene at 250–260 K; on Pt(111), vinyls disproportionate to form ethylidyne ($\text{C}-\text{CH}_3$) and what appears to be acetylide ($\text{C}\equiv\text{CH}$) at 550 K; and on Ni(100), vinyls decompose to acetylene ($\text{HC}\equiv\text{CH}$) at 230 K. Thus, on the three metals that have been studied to date, three different reaction pathways are observed for η^1 -vinyls: coupling on Ag(111), α -C-H bond scission on Pt(111), and β -C-H bond scission on Ni(111).

* Author to whom correspondence should be addressed: telephone, (212) 854-3041; fax, (212) 932-1289; e-mail, bent@chem.columbia.edu.

[⊗] Abstract published in *Advance ACS Abstracts*, June 1, 1996.

In this paper, we present studies of the formation, bonding, and reactions of vinyl groups on a Cu(100) surface. The vinyl groups were generated by thermal dissociation of vinyl bromide and vinyl iodide, and it is shown that, analogous to Ag(111), the only subsequent reaction is coupling to form and evolve butadiene at ~ 250 K. This surface chemistry has been studied by temperature-programmed desorption methods, work function change measurements, and near-edge X-ray absorption fine structure (NEXAFS) spectroscopy. The latter technique provides information on the electronic structure and orientation of the adsorbed species and shows that both vinyl halides and vinyl groups adsorb on Cu(100) with their molecular planes tilted, on average, by $\sim 30^\circ$ and $\sim 40^\circ$ away from the surface, respectively. In both cases, the extent of carbon rehybridization on the copper surface appears to be small. Also, there is no evidence for low-temperature coupling reactions analogous to those observed concurrently with carbon-halogen bond dissociation for iodobenzene on Cu(111)³ and Cu(100).⁴

2. Experimental Section

The experiments were performed in ultra-high-vacuum (UHV) chambers at Columbia University and Brookhaven National Laboratory. The temperature-programmed desorption (TPD) studies and work function change measurements were conducted in a UHV chamber at Columbia University. Detailed descriptions of the system can be found in refs 21 and 22.

The Cu(100) sample (Monocrystals Inc., 1 cm in diameter and 2 mm thick) was fastened to a molybdenum button heater via chromel wire wrapped around the grooved edge of the wafer. The crystal could be heated resistively to 1000 K and cooled conductively by liquid nitrogen to 100 K. The crystal temperature was measured with an alumel-chromel thermocouple inserted into a 0.6 mm diameter hole drilled on the edge of the crystal. Routine surface cleaning was achieved by argon ion sputtering at 850 K for 10 min, bombardment at 450 K for 5 min, followed by annealing at 950 K for 10 min. Surface cleanliness was verified by auger electron spectroscopy and reproducibility of the TPD studies. The quadrupole mass spectrometer for TPD was installed behind a differentially pumped shield with a 2 mm diameter aperture. In the TPD studies, the sample was positioned 2 mm away from the aperture so that only the molecules desorbing from the center of the crystal were detected. The heating rate in TPD experiments was 3 K/s.

Real time work function change measurements as a function of surface temperature were carried out by using a Kelvin Probe (KP 5000, McAllister Technical Services). With this probe, the contact potential difference (CPD) between a reference plate and the surface is determined by a phase-locking method. During measurements, the sample was positioned ~ 1 mm away from the reference plate and heated at a rate of 0.1 K/s. The data acquisition rate was ~ 14 s/point with a standard deviation in repeat measurements of < 3 meV. The work function change ($\Delta\Phi$) with respect to the clean surface was then obtained from

$$\Delta\Phi = \Phi_{\text{ad}} - \Phi_{\text{clean}} = (\Phi_{\text{ref}} - \Phi_{\text{clean}}) - (\Phi_{\text{ref}} - \Phi_{\text{ads}}) = \text{CPD}_{\text{clean}} - \text{CPD}_{\text{ads}}$$

where $\text{CPD}_{\text{clean}}$ is the contact potential difference between the reference plate and the clean surface, and CPD_{ads} is the analogous contact potential difference for the adsorbate-covered surface.

Vinyl bromide (Matheson, 98.5%) was introduced into the chamber through a sapphire leak valve. Exposures are reported

in units of langmuirs [1 langmuir (L) = 1×10^{-6} torr·s]. In these studies, the term “monolayer” (ML) will be used to refer to saturation of the first layer on the surface, as determined from studies of vinyl halide molecular desorption.

NEXAFS measurements were carried out on beamline U1A of the National Synchrotron Light Source at Brookhaven National Laboratory. Details of the apparatus are given in ref 10. The two-stage UHV chamber is equipped with an ion-sputtering gun, an auger electron spectrometer, and a quadrupole mass spectrometer, which allowed TPD results to be reproduced and exposures to be calibrated. All NEXAFS spectra were recorded by using a partial electron yield detector with a retarding voltage of 200 eV. The energy scale was calibrated to set the characteristic $\sigma^*_{\text{C-1}}$ resonance for methyl iodide multilayers at 286.0 eV. The resolution of the monochromator was 0.30 eV. All of the NEXAFS spectra were first normalized by the incident light energy as monitored by a reference grid. The spectra are reported here as the adsorbate-covered surface spectra divided by the clean surface spectra taken at the same incidence angle. The curve-fitting procedure has been fully discussed by Outka and Stöhr.²³

3. Results and Interpretations

We organize and present the results as follows. The thermal desorption/reaction results are discussed first to provide an overview of the chemistry of vinyl halides on the surface. Subsequently, chemical displacement, NEXAFS, and work function change results are presented, and these studies detail the vinyl group formation and reaction kinetics, as well as provide information on the chemical, electronic, and structural properties of the physisorbed vinyl bromide and chemisorbed vinyl groups on the surface.

3.1. Temperature-Programmed Desorption/Reaction Studies. Temperature-programmed desorption (TPD) spectra for the molecular desorption of vinyl bromide ($\text{CH}_2=\text{CHBr}$) from Cu(100) are presented in the top panel of Figure 1, and the peak area as a function of exposure is plotted in the inset. For vinyl bromide exposures below 2.5 langmuirs, no molecular desorption is observed. For exposures between 2.5 and 8 langmuirs, a linear increase in molecular desorption is observed, with a peak maximum at 122 K for an exposure of 8 langmuirs. Molecular desorption shows no increase beyond 8 langmuirs for exposures performed at 110 K. However, an additional molecular desorption peak is observed at ~ 107 K for exposures above 8 langmuirs when the surface is dosed at 100 K. The 107 K peak (not shown here) does not saturate with increasing exposures and is assigned to the desorption of condensed vinyl bromide multilayers on the surface.

For exposures below 2.5 langmuirs, vinyl bromide dissociates on the Cu(100) surface. The sole hydrocarbon product detected is 1,3-butadiene ($\text{CH}_2=\text{CH}-\text{CH}=\text{CH}_2$), and TPD spectra for butadiene are presented in the bottom panel of Figure 1. This product was identified from its ion fragmentation pattern on the basis of a comparison of the relative intensities of the $m/e = 39, 50, 51, 53,$ and 54 ions with reference spectra in the literature.²⁴ No hydrogen desorption is detected at any exposure, and no carbon is detected on the surface by AES for temperatures > 500 K. Bromine left on the surface desorbs in the form of CuBr above 800 K. As shown in Figure 1, the butadiene is evolved from the surface at ~ 250 K. This temperature is close to that for butadiene desorption from Cu(100), but in comparing these results with the 1,3-butadiene TPD spectra shown in Figure 2, there are subtle but significant differences between butadiene evolution from vinyl bromide monolayers and that from

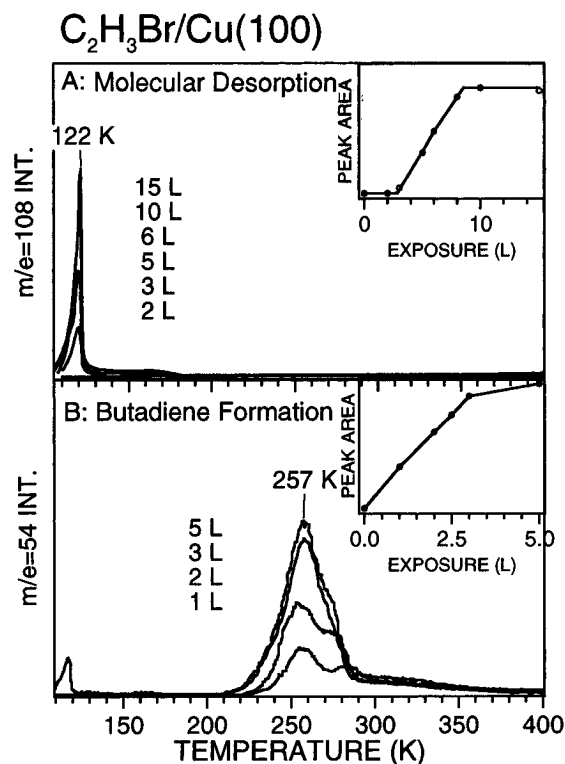


Figure 1. Temperature-programmed reaction/desorption spectra of vinyl bromide (C_2H_3Br) from Cu(100): (A) $m/e = 108$ (C_2H_3Br) evolution; (B) $m/e = 54$ (1,3-butadiene, C_4H_6) evolution. The amounts of C_2H_3Br desorption and C_4H_6 evolution are plotted as a function of exposure in the insets of (A) and (B), respectively. L in this figure represents langmuirs.

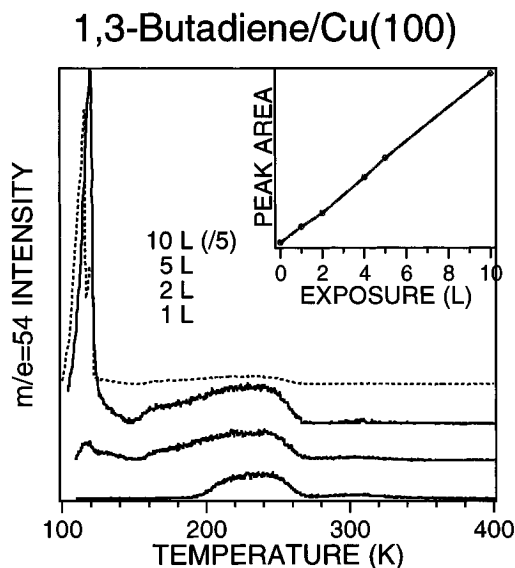


Figure 2. Temperature-programmed desorption spectra of 1,3-butadiene (C_4H_6 , $m/e = 54$) from Cu(100). The amount of C_4H_6 desorbing from the surface is plotted as a function of exposure in the inset. L in this figure represents langmuirs.

butadiene monolayers. In particular, note that for a half-monolayer exposure (~ 1 langmuir) of butadiene, the TPD peak profile shown in Figure 2 is quite broad, extending from 200 to 250 K. By contrast, the onset for butadiene evolution from vinyl bromide is always >210 K, even though the maximum butadiene yield from vinyl bromide is in excess of that for a 1.2 langmuir exposure of butadiene. The implication is that the rate of butadiene evolution from vinyl bromide monolayers

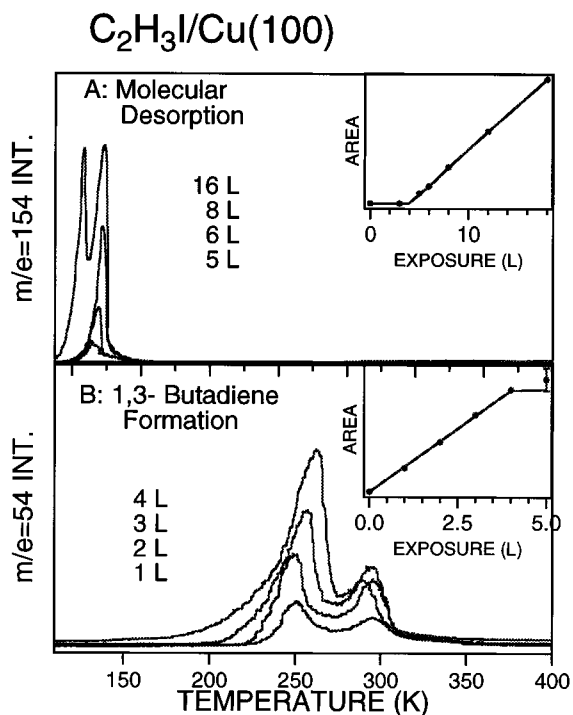


Figure 3. Temperature-programmed reaction/desorption spectra of vinyl iodide (C_2H_3I) from Cu(100): (A) $m/e = 154$ (C_2H_3I) evolution; (B) $m/e = 54$ (1,3-butadiene, C_4H_6) evolution. The amounts of C_2H_3I desorption and C_4H_6 evolution are plotted as a function of exposure in the insets of (A) and (B), respectively.

is, at least in part, determined by the rate at which butadiene is formed.

Thermal desorption results for vinyl iodide are presented in Figure 3. The absence of molecular desorption for exposures below 4.0 langmuirs reflects the thermal dissociation of vinyl iodide molecules on the surface. As for vinyl bromide, the only hydrocarbon product detected for submonolayer exposures is 1,3-butadiene, which desorbs from the surface between 250 and 300 K for an exposure of 4 langmuirs. The similarity in chemistry between vinyl iodide and vinyl bromide on Cu(100) suggests that thermal dissociation of these two vinyl halides produces a common surface intermediate, which is presumably surface vinyl groups. This inference is substantiated by the chemical displacement, NEXAFS, and work function change studies of vinyl bromide presented in the following. All three studies show that vinyl bromide dissociates at ~ 160 K on Cu(100), and the NEXAFS spectra are consistent with the formation of surface vinyl groups. All three series of studies also show that the intermediate formed at 160 K is stable on Cu(100) up to the 210 K temperature where butadiene evolution is first detected. The NEXAFS studies also provide some insights into the geometric and electronic structure of the adsorbed molecules (vinyl bromide) and surface intermediates (vinyl groups).

3.2. Chemical Displacement Studies. Chemical displacement is the term we use to describe the process by which a weakly bonded adsorbate is displaced from the surface by other adsorbates, which preferentially bond to the surface. On copper, this process is quite facile at 100 K for molecules that are adsorbed intact on the surface.²⁵ As a result, stable reactants or products can be displaced at temperatures where they do not desorb, but instead remain adsorbed as multilayers on the surface. A subsequent TPD experiment thus can be used to quantify their coverage from the area of the multilayer TPD peak. In the case of vinyl bromide on Cu(100), we have applied

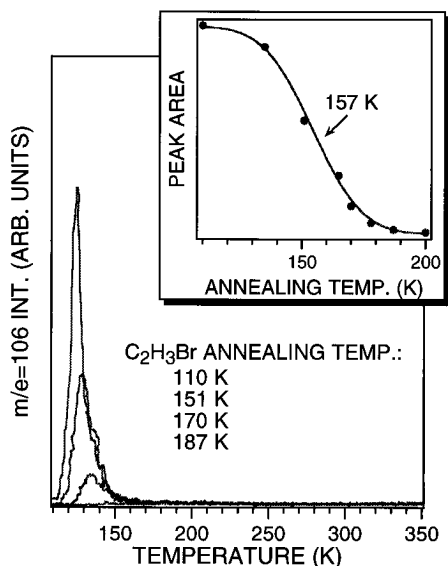


Figure 4. Determination of the C-Br bond dissociation temperature for vinyl bromide on Cu(100) by chemical displacement experiments. 1 ML (2.5 langmuirs) of vinyl bromide was deposited on Cu(100), heated to various temperatures as indicated, and quenched by cooling the crystal to 100 K. Any undissociated vinyl bromide remaining was then displaced by 1 ML (2.5 langmuirs) of benzene. The vinyl bromide TPD spectra were obtained by monitoring $m/e = 106$ (vinyl bromide molecular ion). The inset shows the area of vinyl bromide TPD peak plotted vs annealing temperature to determine the temperature of C-Br bond cleavage.

chemical displacement to monitor the C-Br bond dissociation kinetics.

In these vinyl bromide displacement studies, benzene was used as the displacing agent. While no vinyl bromide desorbs from Cu(100) for exposures less than 2.5 langmuirs in the absence of benzene, we find that 1 ML (2.5 langmuirs) of benzene displaces vinyl bromide (almost quantitatively) from the monolayer to the multilayer. This conclusion is based on the facts that the 120 K peak temperature for the desorption of displaced vinyl bromide from the multilayer is consistent with that observed in Figure 1 for vinyl bromide multilayers and that the yield of butadiene from vinyl bromide dissociation after displacement is decreased by 90%.²⁵

Figure 4 shows results from the application of vinyl bromide displacement by benzene to determine the vinyl bromide dissociation temperature on the surface. In these experiments, the surface (precovered by a monolayer of vinyl bromide) was annealed at different temperatures, and the vinyl bromide molecules remaining on the surface were then displaced by a monolayer of benzene molecules (2.5 langmuirs) at 110 K. Figure 4 shows the vinyl bromide TPD spectra taken after this anneal/quench/displace protocol. As expected, the intensity of vinyl bromide thermal desorption decreases with increasing annealing temperature, reflecting the decrease in the surface vinyl bromide coverage as a result of C-Br dissociation upon annealing to higher temperatures. The inset of Figure 4 presents the vinyl bromide desorption peak area as a function of the annealing temperature. The decrease in peak area as a function of annealing temperature has an inflection point at ~ 157 K, which is indicative of C-Br bond dissociation. Note that the 157 K inflection point is analogous to the peak temperature in a TPD experiment. Studies reported elsewhere show that the anneal/quench protocol used in these experiments is equivalent to a continuous and linear surface heating rate of 0.5 K/s.²²

3.3. Near-Edge X-ray Absorption Fine Structure (NEXAFS) Measurements. Figure 5 presents near-edge X-ray

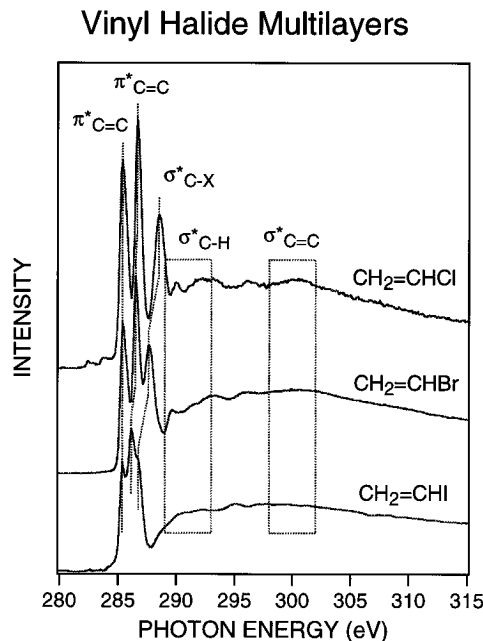


Figure 5. Near-edge X-ray absorption fine structure (NEXAFS) spectra of multilayers of the indicated vinyl halides on Cu(100). The energy values and assignments for the transitions are given in Table 1.

TABLE 1: Assignments of the Near-Edge X-ray Absorption Fine Structure Spectra (Figures 5-8) for Vinyl Halide Multilayers and Vinyl Groups on Cu(100)^a

	$\pi^*_{C=C}, C_1$	$\pi^*_{C=C}, C_2$	σ^*_{C-X}	σ^*_{C-H}	σ^*_{C-H}	$\sigma^*_{C=C}$
CH ₂ =CHCl	285.4	286.8	288.5	290.2	<i>b</i>	300.8
CH ₂ =CHBr	285.4	286.5	287.6	288.5 ^c	289.9 ^c	300.0 ^d
CH ₂ =CHI	285.4	286.2	286.7	<i>b</i>	<i>b</i>	299.0
CH ₂ =CH	285.2	286.3		288.55	290.38	298.0

^a The assignments are based on NEXAFS and EELS spectra for related molecules in the literature (refs 26-29), as well as on the polarization dependencies of the resonances for submonolayers on Cu(100). ^b Resonances cannot be clearly resolved from the limited multilayer results. ^c Monolayer data. ^d The resonance is at 302.0 eV for monolayer.

absorption fine structure (NEXAFS) spectra of vinyl halide (C₂H₃Cl, C₂H₃Br, C₂H₃I) multilayers (~ 10 layers) taken at normal incidence ($\theta = 90^\circ$, where θ is the angle between the direction of propagation of incident synchrotron light and the surface plane). The peak assignments are presented in Table 1. These assignments are made by comparison with NEXAFS and EELS studies of ethylene,²⁶⁻²⁹ fluoroethylenes,²⁹ and chloroethylenes.³⁰

For each of these vinyl halides, three sharp resonances are observed below 290 eV. The lowest energy resonance in all three spectra occurs at 285.4 eV, while the two higher energy resonances differ in energy for the three vinyl halides, shifting to lower energy as the substituted atom is changed from chlorine to bromine to iodine. We assign the two lower energy resonances in each spectrum (one of which is at 285.4 eV in each case) to $C_{1s} \rightarrow \pi^*_{C=C}$ excitations, and the remaining higher energy resonance is attributable to a $C_{1s} \rightarrow \sigma^*_{C-X}$ transition. The existence of two $\pi^*_{C=C}$ excitations for the halogen-substituted ethylenes (ethylene has only one $\pi^*_{C=C}$ resonance)²⁷⁻²⁹ can be attributed to electron excitation from the two different carbon atoms in the molecule—carbons that are inequivalent (in both the initial and final states) due to the halogen substitution at one end of the molecule.^{29,30} The assignment is based on the following observations. The $\pi^*_{C=C}$ resonance at 285.4 eV, which is common to all three vinyl halides, is attributable to the excitation of a carbon 1s electron from the

methylene (CH₂) group to the $\pi^*_{C=C}$ orbital. A similar resonance is observed at 285 eV for vinyl fluoride,²⁹ and the slight difference in energy probably is not significant because of the lack of reference in the energy scales. We also note that the lone π^* resonance for ethylene appears at 284.6 eV in the gas phase²⁶ and on Cu(100).²⁷ The other $\pi^*_{C=C}$ excitation occurs at different energies for the various vinyl halides, decreasing from 286.8 eV in vinyl chloride to 286.5 eV in vinyl bromide to 286.2 eV in vinyl iodide. This resonance corresponds to the excitation of carbon 1s electrons from the CHX group to the $\pi^*_{C=C}$ orbital. The separation between the two $\pi^*_{C=C}$ resonances is consistent with the carbon 1s orbital energy shift upon binding with halogen atoms. The difference is 2.1 eV for vinyl fluoride,²⁹ 1.4 eV for vinyl chloride (see also ref 30), 1.1 eV for vinyl bromide, and 0.8 eV for vinyl iodide. In addition, for each vinyl halide, the C_{1s}(CHX) \rightarrow $\pi^*_{C=C}$ resonance has a larger intensity than the C_{1s}(CH₂) \rightarrow $\pi^*_{C=C}$ resonance. This finding is consistent with prior studies in the literature where it was concluded that the $\pi^*_{C=C}$ resonance intensity increases with increasing degree of halogenation of the carbon atom.^{29,30}

All of these consistencies support our assignment of the vinyl iodide spectrum, where the difference in energy between the C_{1s}(CHX) \rightarrow $\pi^*_{C=C}$ and C_{1s}(CHX) \rightarrow σ^*_{C-X} is only 0.5 eV. Furthermore, the assignment of the 286.4 eV transition in vinyl iodide to a C_{1s}(CHI) \rightarrow $\pi^*_{C=C}$ excitation and the 286.7 eV transition to a C_{1s}(CHI) \rightarrow σ^*_{C-X} excitation, as opposed to the reverse, is supported by the peak positions for the C_{1s}(CHX) \rightarrow σ^*_{C-X} transitions, which are at 288.5 eV for σ^*_{C-Cl} , 287.6 eV for σ^*_{C-Br} , and 286.7 eV for σ^*_{C-I} . Gas phase methyl halides have σ^*_{C-X} resonances at 287.34 (CH₃Cl), 286.48 (CH₃Br), and 285.65 eV (CH₃I). The 1.2 eV shift in absolute energy between the methyl halide and vinyl halide σ^*_{C-X} resonances can be attributed to the different hybridization of carbon atoms and/or an offset between the absolute energy scales. We note, however, that the differences in energies between the σ^*_{C-X} resonances in these two systems are virtually identical, being 0.9 eV between σ^*_{C-Br} and σ^*_{C-Cl} and \sim 0.9 eV between σ^*_{C-I} and σ^*_{C-Br} in both cases.

The polarization dependence of the transitions in the *submonolayer* spectra also supports the multilayer peak assignments. The $\pi^*_{C=C}$ transitions have transition dipole moments perpendicular to the molecular plane, while the σ^*_{C-X} resonances have their transition dipoles within the molecular plane. [On the basis of a heat of adsorption of only 7 kcal/mol for vinyl chloride on Cu(100),³⁰ it is reasonable to presume that the vinyl halide molecules are not significantly rehybridized upon adsorption and that the molecules remain approximately planar.] As will be discussed in more detail later, the vinyl bromide monolayer NEXAFS spectra show a distinct polarization dependence, with the peak at 287.6 eV (σ^*_{C-Br}) having a polarization dependence opposite that of the transitions at 285.4 and 286.5 eV (both $\pi^*_{C=C}$). Studies of vinyl chloride monolayers on the same surface (presented elsewhere)³¹ have also demonstrated opposite angular dependencies between the σ^*_{C-Cl} and $\pi^*_{C=C}$ resonances, as assigned in Table 1.

Figure 6 displays the NEXAFS spectra for 0.8 monolayers of vinyl bromide on Cu(100) at 95 K taken at both grazing ($\theta = 20^\circ$, where θ is the angle between the direction of propagation of synchrotron light and the surface plane) and normal incidence ($\theta = 90^\circ$). Although the spectra show a distinct angular dependence, when both angles of incidence are considered, all the resonances observed in the multilayer spectra are also observed in the monolayer. In particular, the C_{1s} \rightarrow $\pi^*_{C=C}$ transitions are visible at grazing incidence while the C_{1s} \rightarrow

C₂H₃Br/Cu(100)

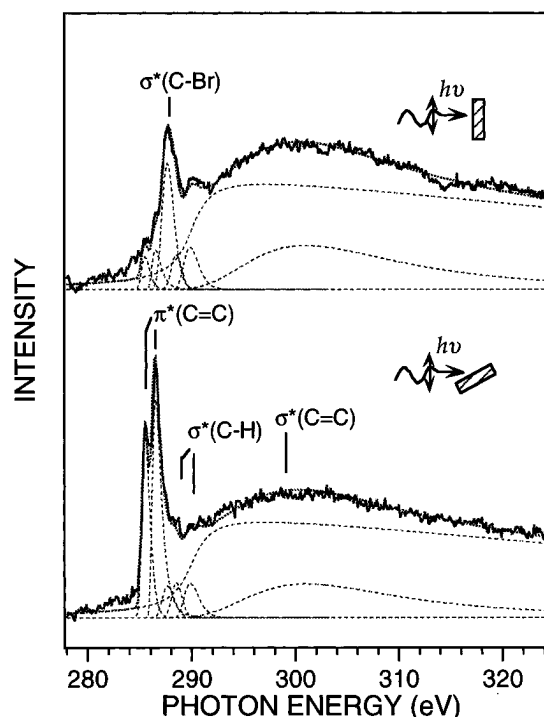


Figure 6. NEXAFS spectra for a vinyl bromide submonolayer on Cu(100). Top panel: NEXAFS spectrum taken at normal incidence ($\theta = 90^\circ$, where θ is the angle between the direction of propagation of the incidence synchrotron light and the surface). Bottom panel: NEXAFS spectrum taken at grazing incidence ($\theta = 20^\circ$). The surface temperature was at 95 K, and the coverage was \sim 0.8 ML (relative to monolayer saturation). The spectral deconvolution is shown as dashed lines.

σ^*_{C-Br} transition is observed at normal incidence. The fact that all transitions are observed indicates that the vinyl bromide molecules remain intact on the surface at 95 K. Further, there is no measurable shift in the resonance positions compared with multilayers, suggesting that physisorption of the molecules on the surface has little effect on the electronic structure of the vinyl bromide molecules.

The polarization dependence of the π^* and σ^* resonances for vinyl bromide indicates that the molecules in the monolayer orient preferentially on the surface. In particular note that the $\pi^*_{C=C}$ resonance is more intense at grazing incidence and the σ^*_{C-Br} and $\sigma^*_{C=C}$ resonances are more intense at normal incidence. If we assume, for the moment, that the geometric and electronic structures of vinyl bromide are unaffected by adsorption, then on the basis of gas phase studies,³² we expect that the transition moment for the $\pi^*_{C=C}$ resonance is directed perpendicular to the molecular plane, while the transition moment for the $\sigma^*_{C=C}$ transition is along the C=C bond and that for the σ^*_{C-Br} transition is along the C-Br bond. Furthermore, all of these resonances are vector (rather than planar) in character (see ref 32 for an explanation of this terminology), so that the orientation of the transition moment with respect to the surface normal can be calculated by comparing the resonance intensities at 90° and 20° angles of incidence. Quantitatively,³²

$$\frac{I(\alpha, \theta = 90^\circ)}{I(\alpha, \theta = 20^\circ)} = \frac{P \sin^2 \alpha + (1 - P) \sin^2 \alpha}{[P(2 \cos^2(20^\circ) \cos^2 \alpha + \sin^2(20^\circ) \sin^2 \alpha) + (1 - P) \sin^2 \alpha]} \quad (1)$$

TABLE 2: NEXAFS Peak Intensity Ratios for 90° and 20° Angles of Incidence [$I(\theta = 90^\circ)/I(\theta = 20^\circ)$] and Orientations (α) of the Indicated Transition Moments with Respect to the Surface Normal

	vinyl bromide			vinyl		
	$\sigma^*_{C=C}$	$\pi^*_{C=C}$	σ^*_{C-Br}	$\sigma^*_{C=C}$	$\pi^*_{C=C}$	σ^*_{C-Cu}
$I(\theta = 90^\circ)/I(\theta = 20^\circ)$	1.3	0.17	4.1	1.1	0.75	
α (deg)	$58 \pm 3^\circ$	$28 \pm 5^\circ$	$83 \pm 3^\circ$	$56 \pm 3^\circ$	$50 \pm 3^\circ$	

where I is the peak intensity, α is the angle between the molecular plane and the surface, θ is the angle between the direction of propagation of the incident light and the surface, and P is the degree of polarization of synchrotron light.

The deconvolution of the resonances in the submonolayer vinyl bromide spectra (which was used in evaluating eq 1) is shown in Figure 6 by the dashed lines. Note that, although an energy difference of 1.1 eV between the two carbon 1s orbitals is indicated by the split of the $C_{1s} \rightarrow \pi^*_{C=C}$ resonances, only one carbon edge has been applied to fit the data. This single-edge function can be regarded as an average of the two carbon edges. Note also that the same peak positions and widths were used in deconvoluting both the grazing and the normal incidence spectra in Figure 6; only the relative peak intensities have been varied in making these two deconvolutions.

By using these curve fits and taking a polarization purity (P) of 0.85, we obtain the angles of inclination, α , given in Table 2. On the basis of these values for the orientations of the transition moments, we can determine the molecular orientation (assuming the molecule maintains its planarity upon adsorption). We begin by recognizing that if one starts with vinyl bromide oriented with the molecular plane parallel to the surface, one can arrive at any possible tilted configuration by first rotating the vinyl bromide about the axis A_1 that is defined by the C=C bond and then rotating about the orthogonal axis A_2 that is also parallel to the surface. We can then use elementary vector analysis to derive an expression (not shown) that describes how the molecule must rotate about these two axes such that the angle that the σ^*_{C-Br} transition moment makes with the normal is consistent with the measured value of 83° . Now, if one examines all of the possible combinations of rotations about A_1 and A_2 that are subject to the constraint that the σ^*_{C-Br} transition moment is 83° with respect to the normal, one finds that there is only one combination that will give an orientation such that the calculated angles between the $\pi^*_{C=C}$ and $\sigma^*_{C=C}$ transition moments and the surface normal agree with the angles measured in the NEXAFS experiments. A schematic diagram of a vinyl bromide molecule with this orientation relative to the surface is shown in Figure 7. It should be noted that since the orientation shown in Figure 7 represents a monolayer average, it is possible that the majority of the molecules lie essentially flat on the surface and that the nonzero value for the degree of tilt is due to a small fraction of molecules bonding with a tilted angle on surface defect sites.

NEXAFS spectra can also provide some insight into the extent to which the bonding within the vinyl bromide molecule is affected by coordination to the surface. Specifically, an empirical linear relationship between the C—C bond length in hydrocarbons and their σ^* shape resonance energy position has been reported in the literature.^{27,28,33–36} Although caution should be taken in the application of this empirical correlation,³⁷ a variety of studies have shown that this correlation is valid for simple hydrocarbons.^{27,28,33–36} For chemisorbed molecules, the σ^* shape resonance position is defined as the difference between the resonance energy and the ionization potential (IP). As noted in refs 28, 33, and 34, for simple hydrocarbon molecules, the

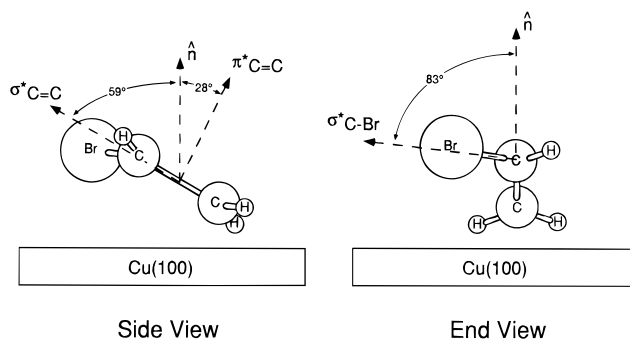


Figure 7. Schematic diagram of a vinyl bromide molecule oriented on the Cu(100) surface as viewed from the side and the end. This orientation is such that the angles that the $\pi^*_{C=C}$, $\sigma^*_{C=C}$, and σ^*_{C-Br} transition moments make with the normal are consistent with the ones measured in the NEXAFS experiments. In particular note that the vector that represents the $\pi^*_{C=C}$ transition moment is rotated by $\sim 9^\circ$ out of the plane defined by the surface normal vector and the vector that represents the $\sigma^*_{C=C}$ transition, bringing the Br atom slightly closer to the surface.

reference energies are insensitive to the type of hydrocarbon. As a result, it is possible to simply use the energy of the σ^* resonance to derive intramolecular bond lengths. As shown in Figure 5, the $\sigma^*_{C=C}$ resonance for vinyl bromide multilayers is at 302 eV. According to a plot of the σ^* resonance position as a function of C—C distance presented in ref 28, this energy correlates with a C—C distance of $1.33 \pm 0.02 \text{ \AA}$, which is the same as the distance for C=C double bonds in gas phase ethylene.³⁸ As shown in Figure 6, vinyl bromide monolayers have a σ resonance at 300 eV, which corresponds to a C—C distance of $1.37 \pm 0.02 \text{ \AA}$. A similar small increase in the C=C bond distance has also been determined previously by NEXAFS for ethylene monolayers on Cu(100).²⁷ These hundredths of an angstrom increases in bond length are much smaller than the bond lengthening for ethylene in monolayers on Pt(111),³⁴ where the C—C distance reaches 1.49 \AA for di- σ coordination of the molecules.

NEXAFS spectra of vinyl bromide monolayers as a function of surface temperature corroborate the chemical displacement studies showing C—Br dissociation at 160 K. These spectra also provide evidence for the formation of surface vinyl groups. Figure 8 presents NEXAFS spectra taken at both normal and grazing incidences after annealing a vinyl bromide monolayer at 210 K. The absence of the σ^*_{C-Br} resonance at 287.6 eV at both incidence angles indicates that C—Br bond dissociation has occurred below 210 K. In addition, the fact that all other resonances ($\pi^*_{C=C}$, σ^*_{C-H} , and $\sigma^*_{C=C}$) are still observed at virtually the same energies at 210 K provides strong evidence for the formation of surface vinyl groups that have an electronic structure very similar to that for the vinyl halides. In particular note that the σ^* resonance is at 298 eV, which indicates a C—C separation of $1.39 \pm 0.02 \text{ \AA}$. This distance is slightly longer than that in vinyl bromide, but it is still significantly less than the C—C single bond distance in ethane of 1.53 \AA .³⁸ We also note that the split in the $\pi^*_{C=C}$ resonance observed for vinyl halides, which reflects the chemical inequality of the two carbon atoms, is also observed for the surface vinyl groups. The split of 1.1 eV between the two $\pi^*_{C=C}$ resonances for vinyl is the same as that for vinyl bromide, suggesting that the electronic effect of the copper surface is similar to that of a bromine atom. By contrast, for vinyl chloride and vinyl iodide, the splitting of the $\pi^*_{C=C}$ resonance is 1.4 and 0.8 eV, respectively, while for vinyl groups on Ni(100) the splitting is 2.5 eV.⁵

Unlike the spectra for molecular vinyl bromide, variation in the incidence angle of the synchrotron light has little effect on

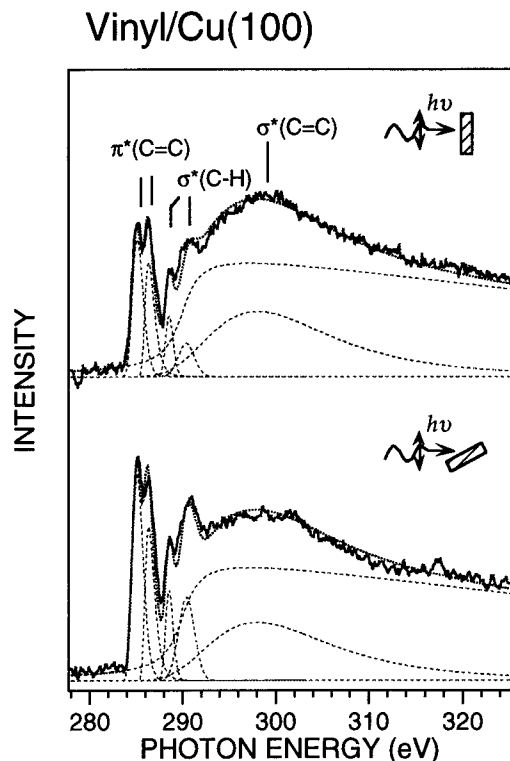


Figure 8. NEXAFS spectra for a submonolayer of vinyl groups on Cu(100) at glancing ($\theta = 20^\circ$) and normal ($\theta = 90^\circ$) angles of incidence. The vinyl groups were generated by heating a surface precovered by 0.8 ML of vinyl bromide to 210 K. The spectral deconvolution is shown as dashed lines.

the peak intensities of the $\pi^*_{C=C}$ resonances for surface vinyl groups. This weak angular dependence of the $\pi^*_{C=C}$ resonance intensities indicates (according to eq 1) that the C=C bond is tilted at an angle of $56 \pm 3^\circ$ from the surface normal, while the molecular plane is tilted at an angle of $\sim 50 \pm 3^\circ$ from the normal. This tilted orientation probably reflects a compromise between a direct carbon-metal σ bond and attractive interactions between the C=C bond and the surface. This configuration is consistent with the conclusions from NEXAFS studies of vinyl groups on Ni(100).⁵ The orientation is also analogous to that for phenyl groups (C_6H_5) on Cu(111), where a tilt angle of $\sim 45^\circ$ (from the surface plane) was observed.² All of these geometries reflect surface coverages near saturation of the monolayer; the coverage dependence of this tilting has yet to be investigated.

Figure 9 compares vinyl bromide monolayer spectra taken at 95 and 210 K, both at normal incidence. As mentioned earlier, and as is clear from these spectra, the σ^*_{C-Br} resonance is visible at 95 K, but disappears by 210 K due to the dissociation of the C-Br bond. Monitoring of the disappearance of the σ^*_{C-Br} resonance as a function of surface temperature allows us to measure C-Br bond dissociation kinetics. The inset in Figure 9 presents the σ^*_{C-Br} peak intensity as a function of annealing temperature. In determining these intensities, the σ^*_{C-Br} peak has been normalized by the carbon edge, whose height is proportional to the amount of carbon on the surface. Since thermal desorption studies show that no species are liberated from the surface below 210 K for vinyl bromide monolayers, the surface carbon coverage remains constant, and the normalized σ^*_{C-Br} peak intensity is simply a measure of the number of vinyl bromide molecules remaining on the surface. Although some experimental uncertainty is introduced by this normalization procedure, a decrease in the σ^*_{C-Br} signal is clearly observed with a maximum rate at ~ 160 K. This temperature is consistent with the C-Br bond dissociation

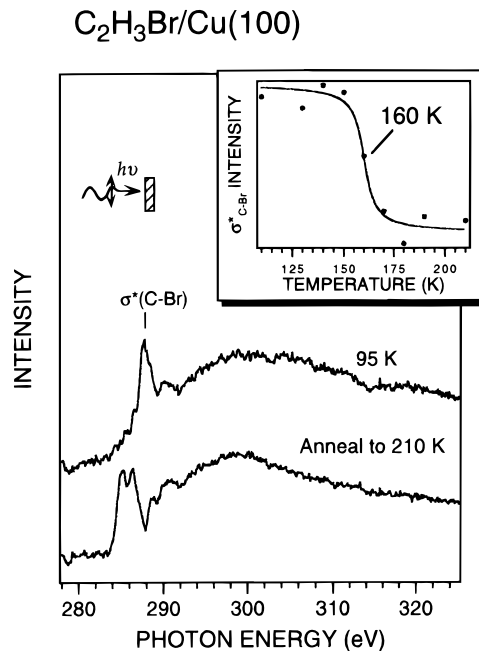


Figure 9. Determination of the C-Br bond dissociation temperature in vinyl bromide on Cu(100) by NEXAFS. 0.8 ML of vinyl bromide was deposited on Cu(100) and heated to various temperatures, and the NEXAFS spectra were taken at normal incidence. The inset shows the σ^*_{C-Br} resonance intensity plotted vs annealing temperature to determine the temperature of C-Br bond dissociation.

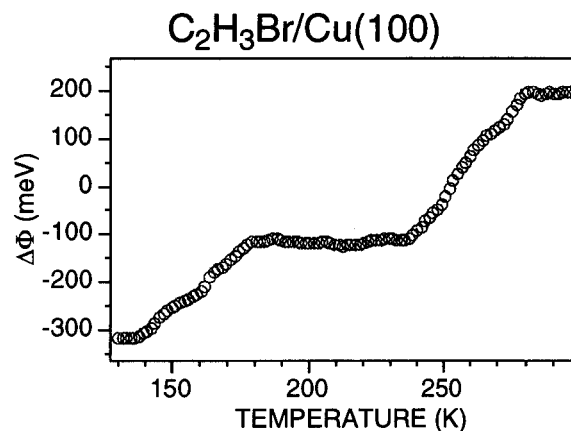


Figure 10. Temperature-programmed surface work function change measurements for a submonolayer of vinyl bromide on Cu(100). The surface coverage is ~ 0.8 ML. The heating rate in the study was 0.1 K/s.

temperature of 157 K determined from the chemical displacement experiments.

3.4. Work Function Change Measurements. Changes in the coverage, bonding, and structure of adsorbates on surfaces are generally accompanied by changes in the surface work function. In the present studies, the surface work function change was measured in real time as a function of surface temperature to monitor the surface reactions. Figure 10 displays the work function change as a function of temperature when 0.8 monolayer of vinyl bromide on Cu(100) is heated at a rate of 0.1 K/s. As shown in the figure, the adsorption of vinyl bromide at 110 K induces a surface work function decrease of 300 meV. This decrease is typical for the adsorption of polar halogenated hydrocarbons on metal surfaces.^{21,22,39,40} Upon heating of the crystal, two work function increases are observed for temperatures below 350 K: a 200 meV increase between 140 and 175 K and a 300 meV increase between 240 and 280 K. These work function changes are indicative of C-Br bond

dissociation and butadiene evolution, respectively. Increases in the work function upon carbon–halogen bond dissociation^{22,39,40} and alkene evolution²² have been observed in previous studies on metals. Above 300 K, with only bromine atoms left on the surface, the surface work function is 200 meV higher than the value of clean Cu(100). This result is consistent with previous observations that halogen atom-terminated metal surfaces tend to have slightly higher work functions than the clean surface.^{22,39,40}

Since the surface work function is constant to within 10 meV from 180 to 240 K, we can conclude with confidence that the species formed on the surface by C–Br bond dissociation at 160 K is thermally stable up to 240 K, where butadiene is evolved to the gas phase. On the basis of the TPD and NEXAFS results, we conclude that this surface intermediate is vinyl.

4. Discussion

The preceding results establish that vinyl bromide, which bonds to Cu(100) with its molecular plane within $\sim 30^\circ$ of parallel to the surface, dissociates at ~ 160 K to form surface vinyl groups, which subsequently couple at ~ 250 K to form and evolve butadiene from the surface. The NEXAFS spectra suggest that the amount of rehybridization in both adsorbed vinyl bromide and surface vinyl groups is minimal compared with that in multilayers. The NEXAFS spectra also show that vinyl groups bond to Cu(100) with their C=C bonds tilted away from the plane of the surface by $56 \pm 3^\circ$. In the discussion that follows, the vinyl coupling reaction and the lack of vinyl dehydrogenation on Cu(100) are discussed in light of results for other metals and for other hydrocarbon fragments.

Vinyl coupling on copper is analogous to vinyl coupling on silver.⁷ Both processes occur at similar temperatures to produce butadiene with 100% selectivity for submonolayer coverages. There is, though, a 40 K higher temperature for vinyl coupling on Ag(111)¹⁵ than on Cu(100) (this work), which is consistent with the 40 K higher temperature for phenyl coupling on Ag(111)⁴¹ than on Cu(111).^{3,21} This trend, however, is opposite the trend found for methyl coupling on copper and silver. On Ag(111), methyl groups couple to form ethane at 190–200 K,³⁹ while on Cu(111), coupling is only observed at high coverages and only for temperatures above 420 K.⁴⁰ A recent comparison of the literature data for alkyl coupling and for methyl radical desorption has suggested that the relative rates of alkyl coupling on metal surfaces are a direct reflection of the relative metal–alkyl bond strengths.⁴² If a similar correlation is true for vinyl and phenyl, then the vinyl and phenyl bond energies on silver are stronger relative to the alkyls than on copper.

In comparing the rates of vinyl bromide coupling and phenyl coupling on Cu(100), we find some interesting differences. At low surface coverages where vinyl and phenyl groups can be formed and isolated on the surface, vinyl groups couple at 100 K lower temperature than phenyl groups. On the other hand, at high surface coverages, iodobenzene coupling to form biphenyl is detected at temperatures below 200 K, but there is no evidence for such a facile, low-temperature pathway in the case of vinyl bromide on Cu(100). This low-temperature biphenyl formation pathway has been correlated with a direct reaction between phenyl groups and tilted iodobenzene molecules, which are present at high surface coverages. The absence of a similar low-temperature channel for vinyl bromide coupling may reflect the fact that an analogous high-coverage, tilted orientation is not observed for vinyl bromide.

With respect to the higher coupling temperature for phenyl vs vinyl groups at low coverages on Cu(100), we note that the

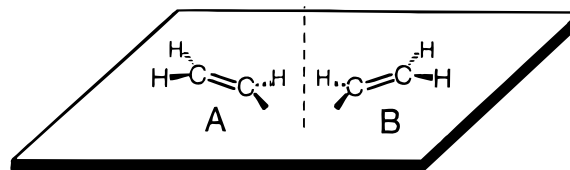


Figure 11. Schematic diagram of the tilted bonding geometry indicated by NEXAFS for vinyl groups on Cu(100). Two enantiomers (A and B) are shown to illustrate the chirality that exists for tilted vinyl groups on the surface.

100 K difference in reaction temperature (350 vs 250 K) corresponds to a difference in activation energy of ~ 6 kcal/mol (for an assumed pseudo-first-order prefactor of 10^{13} s^{-1}), which in turn translates into a difference of about 4 orders of magnitude in rate if the rates are extrapolated to a common temperature of 300 K. This difference probably reflects a number of factors, including a stronger phenyl–copper bond than vinyl–copper and the possible presence of a steric barrier in the case of phenyl coupling since the two rings in the resulting biphenyl (in the gas phase) are canted relative to one another⁴³ to avoid repulsion between the H atoms adjacent to the C–C bond between rings. The lowest energy conformer for butadiene, on the other hand, is planar, so that steric repulsion with the planar surface during coupling will be minimized.

The potential effects of stereochemistry on the vinyl coupling reaction should also be mentioned. While vinyl groups are not chiral in the gas phase, once they bond on the surface in a tilted orientation, as evidenced by the NEXAFS results and as shown schematically in Figure 11, they become chiral, and mirror image structures are not superimposable. The significance of this chirality for the vinyl coupling reaction is unknown at present, but one might expect an effect since the coupling of vinyl groups with the same chirality leads directly to *trans*-butadiene, while the coupling of the mirror image species produces *cis*-butadiene, and the *cis*- and *trans*-butadiene isomers have a small, but significant, energy difference of 2–3 kcal/mol in the gas phase^{44,45} (note that a difference of only 1 kcal/mol in activation energy corresponds to a difference of about an order of magnitude in rate at the temperature of this coupling reaction). A possible manifestation of these chiral coupling effects would be a two-peak structure in TPR analogous to what is observed here for butadiene formation from both vinyl bromide and vinyl iodide (see Figures 1 and 3). Specifically, if we refer to the two chiral vinyl isomers on the surface as A and B, then even if there are equal numbers of A and B species and if only A + A and B + B coupling occurs to give the most stable *trans*-butadiene, a two-peak structure is possible in TPR studies as a result of reaction-induced phase segregation on the surface. This effect is discussed and simulated in refs 46 and 47, and the basic idea is that if diffusion of the A and B species is not sufficiently rapid compared to the rate of coupling (especially in the presence of coadsorbates, such as halogen atoms, in our case), then preferential reaction of A/A and B/B pairs results in A/B islands that react more slowly and give rise to a higher temperature TPR peak. Further studies are needed to confirm whether or not chirality plays a role in the two-peak TPR structure observed for vinyl coupling. The role of coadsorbed halogens also deserves study since vinyl coupling in the absence of halogens on Ag(111)^{19,20} does not produce an analogous two-peak structure.

Finally, we comment briefly on the lack of vinyl decomposition on Cu(100). The lack of dehydrogenation by vinyl groups on Cu(100) is consistent with the absence of C–H bond breaking on Ag(111), but this result is quite different from the facile (< 200 K) α -C–H bond breaking that is concluded for

vinyl on Pt(111)⁴⁸ and the facile (230 K) β -C-H bond breaking that is observed for vinyl on Ni(100).⁵⁻⁷ Alkyl groups readily undergo β -hydride elimination on Cu(100).²² Vinyl groups, however, couple above 250 K on Cu(100) with no β elimination. As a result, we can conclude that β elimination from vinyl is slower than β -hydride elimination from alkyls. This difference may reflect, in part, the orientational rigidity of surface vinyl groups compared with surface alkyls. Recent studies have shown that conformation plays a large role in determining the rate of β elimination from alkyl groups,²² and since one might expect a significant energy barrier for reorienting vinyl, achieving the adsorbate/surface geometry that minimizes the energy required for the β -elimination pathway may be much higher for vinyl than for alkyl groups. A similar barrier for reorientation may also account for the stability of the β -C-H bonds in phenyl groups to temperatures above 300 K on Cu(100).⁴⁹

5. Summary

Our results show that monolayers of vinyl bromide and vinyl iodide dissociate on Cu(100) to produce adsorbed vinyl groups. Chemical displacement studies, NEXAFS experiments, and real time work function change measurements indicate that the C-Br bond cleavage occurs at 160 K in the vinyl bromide monolayer. Vinyl groups are thermally stable up to 250 K where coupling occurs to produce 1,3-butadiene, which also desorbs from the surface at this temperature. NEXAFS studies indicate that monolayer vinyl bromide molecules are oriented with their molecular planes within $\sim 30^\circ$ of parallel to the surface. By contrast, vinyl groups are tilted away from the surface plane. The NEXAFS spectra for both vinyl bromide and vinyl show a splitting of the $\pi^*_{C=C}$ resonance, which is not observed for ethylene. This splitting is attributed to a core level energy difference between the two carbon atoms due to bonding of one carbon with either the bromine or the copper surface.

Acknowledgment. Financial support from the Dow Chemical Corporation, the National Science Foundation (Grant No. CHE-93-18625), and the Camille and Henry Dreyfus Foundation is gratefully acknowledged.

References and Notes

- Zhou, X.-L.; White, J. M. *J. Am. Chem. Soc.* **1992**, *114*, 2031.
- Yang, M. X.; Xi, M.; Yuan, H.; Bent, B. E.; Stevens, P. A.; White, J. M. *Surface Sci.* **1995**, *341*, 9.
- Xi, M.; Bent, B. E. *J. Am. Chem. Soc.* **1993**, *115*, 7426.
- Kash, P. W.; Xi, M.; Sun, D.-H.; Flynn, G. W.; Bent, B. E. Manuscript in preparation.
- Zaera, F.; Fischer, D. A.; Carr, R. G.; Gland, J. L. *J. Chem. Phys.* **1988**, *89*, 5335.
- Zaera, F.; Hall, R. B. *J. Phys. Chem.* **1987**, *91*, 4318.
- Zaera, F.; Hall, R. B. *Surface Sci.* **1987**, *180*, 1.
- Hall, R. B.; Bares, S. J.; DeSantolo, A. M.; Zaera, F. *J. Vac. Sci. Technol. A* **1986**, *4*, 1493.
- Zhu, X.-Y.; Castro, M. E.; Akhter, S.; White, J. M.; Houston, J. E. *Surface Sci.* **1988**, *207*, 1.
- Fischer, D. A.; Colbert, J.; Gland, J. L. *Rev. Sci. Instrum.* **1989**, *60*, 1596.
- Clarke, T. A.; Gay, I. D.; Law, B.; Mason, R. *Faraday Discuss. Chem. Soc.* **1975**, *60*, 119.
- Stuve, E. M.; Brundle, C. R. *Surface Sci.* **1985**, *152/153*, 532.
- Lehwald, S.; Ibach, H. *Surface Sci.* **1979**, *89*, 425.
- Parmeter, J. E.; Weinberg, W. H. *J. Am. Chem. Soc.* **1987**, *109*, 72.
- Zhou, X.-L.; White, J. M. *J. Phys. Chem.* **1991**, *95*, 5575.
- Liu, Z.; Zhou, X.-L.; Buchanan, D. A.; Kiss, J.; White, J. M. *J. Am. Chem. Soc.* **1992**, *114*, 2031.
- Zaera, F.; Bernstein, N. *J. Am. Chem. Soc.* **1994**, *116*, 4881.
- Zhou, X.-L.; Liu, Z.-M.; White, J. M. *Chem. Phys. Lett.* **1992**, *195*, 618.
- Zhou, X.-L.; Schwaner, A. L.; White, J. M. *J. Am. Chem. Soc.* **1993**, *115*, 4309.
- Zhou, X.-L.; White, J. M. *J. Phys. Chem.* **1992**, *96*, 7703.
- Xi, M.; Bent, B. E. *Surface Sci.* **1992**, *278*, 19.
- Tepliyakov, A. V.; Bent, B. E. *J. Am. Chem. Soc.* **1995**, *117*, 10076.
- Outka, D. A.; Stöhr, J. *J. Chem. Phys.* **1988**, *86*, 3539.
- Heller, S. R.; Milne, G. W. A. *EPA/NIH Mass Spectral Data Base*; U.S. Department of Commerce: Washington, DC, 1978; Vol. 1.
- Kash, P. W.; Yang, M. X.; Tepliyakov, A. V.; Flynn, G. W.; Bent, B. E. Manuscript in preparation.
- Hitchcock, A. P.; Brion, C. E. *J. Electron Spectrosc. Relat. Phenom.* **1977**, *10*, 317.
- Arvanitis, D.; Baberschke, K.; Wenzel, L.; Döbler, U. *Phys. Rev. Lett.* **1986**, *57*, 3175.
- Arvanitis, D.; Döbler, U.; Wenzel, L.; Baberschke, K.; Stöhr, J. *Surface Sci.* **1986**, *178*, 686.
- McLaren, R.; Clark, S. A. C.; Ishii, I.; Hitchcock, A. P. *Phys. Rev. A* **1987**, *36*, 1683.
- Cassuto, A.; Hugenschmit, M. B.; Parent, P.; Laffon, C.; Tourillon, H. G. *Surface Sci.* **1994**, *310*, 390.
- Yang, M. X.; Kash, P. W.; Sun, D.-H.; Bent, B. E.; Bare, S.; Holbrook, M.; Fischer, D. A.; Gland, J. L. *Surf. Sci.*, submitted.
- Stöhr, J. *NEXAFS Spectroscopy*; Springer Verlag: New York, 1992; Vol. 25.
- Hitchcock, A. P.; Beaulieu, S.; Sheel, T.; Stöhr, J.; Sette, F. *J. Chem. Phys.* **1984**, *80*, 3927.
- Stöhr, J.; Sette, F.; Johnson, A. L. *Phys. Rev. Lett.* **1984**, *53*, 1684.
- Sette, F.; Stöhr, J.; Hitchcock, A. P. *J. Chem. Phys.* **1984**, *81*, 4906.
- Koestner, R. J.; Stöhr, J.; Gland, J. L.; Horsley, J. A. *Chem. Phys. Lett.* **1984**, *105*, 332.
- Piancastelli, M. N.; Lindle, D. W.; Ferrett, T. A.; Shirley, D. A. *J. Chem. Phys.* **1987**, *86*, 2765.
- Tables of Interatomic Distances*; Chem. Soc. of London: London, 1958.
- Zhou, X.-L.; Solymosi, F.; Blass, P. M.; Cannon, K. C.; White, J. M. *Surface Sci.* **1989**, *219*, 294.
- Lin, J.-L.; Bent, B. E. *J. Vac. Sci. Technol. A* **1992**, *10*, 2202.
- Zhou, X.-L.; Castro, M. E.; White, J. M. *Surface Sci.* **1990**, *238*, 215.
- Paul, A.; Yang, M. X.; Bent, B. E. *Surface Sci.* **1993**, *297*, 327.
- Suzuki, H. *Bull. Chem. Soc. Jpn.* **1959**, *32*, 1340.
- Bock, C. W.; George, P.; Trachtman, M.; Zanger, M. *J. Chem. Soc., Perkin Trans. 2* **1979**, 26.
- Kao, J. *J. Am. Chem. Soc.* **1987**, *109*, 3824.
- Becker, O. M.; Ben-Nun, M.; Ben-Shaul, A. *J. Phys. Chem.* **1991**, *95*, 4803.
- Becker, O. M.; Silverberg, M.; Ben-Shaul, A. *Isr. J. Chem.* **1990**, *30*, 179.
- Zhou, X.-L.; Liu, Z.-M.; White, J. M. *Chem. Phys. Lett.* **1992**, *195*, 618.
- Kash, P. W.; Xi, M.; Sun, D.-H.; Flynn, G. W.; Bent, B. E. *J. Phys. Chem.*, submitted.

JP952386J